Congenital Hyperinsulinism and Glucose Hypersensitivity in Homozygous and Heterozygous Carriers of Kir6.2 (*KCNJ11*) Mutation V290M Mutation

K_{ATP} Channel Inactivation Mechanism and Clinical Management

Karen J. Loechner,[1] Alejandro Akrouh,[2] Harley T. Kurata,[2] Carlo Dionisi-Vici,[3] Arianna Maiorana,[3] Milena Pizzoferro,[4] Vittoria Rufini,[5] Jean de Ville de Goyet,[6] Carlo Colombo,[7] Fabrizio Barbetti,[7,8] Joseph C. Koster,[2†] and Colin G. Nichols[2]

OBJECTIVE—The ATP-sensitive K^+ channel (K_{ATP}) controls insulin secretion from the islet. Gain- or loss-of-function mutations in channel subunits underlie human neonatal diabetes and congenital hyperinsulinism (HI), respectively. In this study, we sought to identify the mechanistic basis of K_{ATP}-induced HI in two probands and to characterize the clinical course.

RESEARCH DESIGN AND METHODS—We analyzed HI in two probands and characterized the course of clinical treatment in each, as well as properties of mutant K_{ATP} channels expressed in COSm6 cells using Rb efflux and patch-clamp methods.

RESULTS—We identified mutation V290M in the pore-forming Kir6.2 subunit in each proband. In vitro expression in COSm6 cells supports the mutation resulting in an inactivating phenotype, which leads to significantly reduced activity in intact cells when expressed homomerically, and to a lesser extent when expressed heteromerically with wild-type subunits. In one heterozygous proband, a fluoro-DOPA scan revealed a causal focal lesion, indicating uniparental disomy with loss of heterozygosity. In a second family, the proband, homozygous for the mutation, was diagnosed with severe diazoxide–unresponsive hypersinsulinism at 2 weeks of age. The patient continues to be treated successfully with octreotide and amlodipine. The parents and a male sibling are heterozygous carriers without overt clinical HI. Interestingly, both the mother and the sibling exhibit evidence of abnormally enhanced glucose tolerance.

CONCLUSIONS—V290M results in inactivating K_{ATP} channels that underlie HI. Homozygous individuals may be managed medically, without pancreatectomy. Heterozygous carriers also show evidence of enhanced glucose sensitivity, consistent with incomplete loss of K_{ATP} channel activity. ***Diabetes*** **60:209–217, 2011**

The ATP-sensitive K^+ channel (K_{ATP}) regulates insulin secretion from the pancreatic β-cell by coupling changes in metabolism to changes in electrical activity. K_{ATP} overactivity suppresses insulin release and causes neonatal diabetes (1,2), whereas K_{ATP} underactivity causes hypersecretion and congenital hyperinsulinemia (HI) (3–5).

HI mutations can cause aberrant channel synthesis or trafficking or altered channel gating (5,6). Mature K_{ATP} channels are hetero-octomers of four pore-forming Kir6.2 subunits (*KCNJ11*) and four sulfonylurea receptor subunits (*ABCC8*) (7–9). We report a novel Kir6.2 mutation (V290M), identified in two unrelated HI probands. V290M reduces channel activity by causing an inactivating phenotype, which explains the HI outcome. Importantly, the V290M mutation is present in the homozygous state in one of the HI-affected probands and is heterozygous in the unaffected parents and one sibling. Oral glucose tolerance tests (OGTTs) on the heterozygous mother and sibling suggest hyper-responsivity in both individuals.

RESEARCH DESIGN AND METHODS

Genetics and molecular biology. Genomic DNA was isolated from whole blood using the DNeasy Tissue Isolation kit (Qiagen, Valencia, CA). KCNJ11 was amplified by PCR and directly sequenced. The identified V290M mutation was engineered into mouse Kir6.2 cDNA in pCMV6B using the Quikchange site-directed mutagenesis kit (Stratagene, La Jolla, CA) and was confirmed by direct sequencing.

Clinical studies. Oral glucose tolerance tests (OGTTs): D-glucose was given orally and blood drawn via peripheral intravenous at baseline and then at hourly intervals. Samples were assayed for serum glucose, insulin, and proinsulin at the Mayo Clinical Laboratory (Rochester, MN). For the mother, the glucose load (Glucola) was 75 g. For the sibling child, the load was 1 g/kg, and the duration of the OGTT was truncated to 3 h due to age. Of note, behavioral changes (e.g., hunger, lethargy) that often followed a meal were reported for the sibling. Given that heterozygous K_{ATP} channel mutations have been identified in patients with HI (6), the mother requested testing for her

From the [1]Department of Pediatrics, University of North Carolina School of Medicine, Chapel Hill, North Carolina; the [2]Department of Cell Biology and Physiology, Washington University School of Medicine, St. Louis, Missouri; the [3]Unit of Metabolic Diseases, Department of Pediatrics, Bambino Gesù Children's Hospital, Rome, Italy; the [4]Unit of Nuclear Medicine, Department of Radiology, Bambino Gesù Children's Hospital, Rome, Italy; the [5]Department of Nuclear Medicine, Catholic University of the Sacred Heart, Rome, Italy; the [6]Department of Surgery, Bambino Gesù Children's Hospital, Rome, Italy; the [7]Laboratory of Monogenic Diabetes, Bambino Gesù Children's Hospital Istituto Di Ricovero e Cura a Carattere Scientifico, Rome, Italy; and the [8]Department of Internal Medicine, University of Tor Vergata, and Laboratory of Monogenic Diabetes, Bambino Gesù Children's Hospital Istituto Di Ricovero e Cura a Carattere Scientifico, Rome, Italy.

Corresponding authors: Colin G. Nichols, cnichols@wustl.edu, and Fabrizio Barbetti, mody.2@libero.it.

Received 22 May 2010 and accepted 15 October 2010. Published ahead of print at http://diabetes.diabetesjournals.org on 27 October 2010. DOI: 10.2337/db10-0731.

K.J.L. and A.A. contributed equally to this study.

†Deceased.

and her son. This case report was submitted to the institutional review board at the University of North Carolina and was declared exempt.

Continuous glucose monitoring system (CGMS): Due to parental wishes to decrease the frequency of octreotide injections, medical therapy was adjusted while monitoring under CGMS as an off-label use. A sensor was placed on three separate occasions for Proband 1 (CareLink; Medtronic MiniMed) after application of topical anesthetic. Medtronic (Caremark) provided training to the parents on how to use devices and mark events such as medication and meals, as well as to corroborate hypoglycemic (sensor set at <80) or hyperglycemic (>200) events detected by an external blood glucose meter. Reference ranges were chosen for the alarm settings to avoid hypoglycemia and minimize glycosuria, as well as to avoid excessive finger sticks for the child. Sensors were placed for a maximum of 5 days and corresponded to periods when treated with *1*) octreotide alone or *2*) octreotide + amlodipine. Of note, the child was tapered off amlodipine while on CGMS for a period of 2 weeks. After monitoring with octreotide alone, amlodipine (0.1 mg/kg divided twice daily) was reintroduced for 5 days prior to CGMS testing. Baseline glucose levels and excursions (high and low) were documented on a continuous basis to evaluate the safety and efficacy of the two treatment regimens.

Fluoro-DOPA analysis of pancreas. Fluoro-DOPA (^{18}F-L-DOPA) positron emission tomography/computed tomography study (4 MBq/Kg of ^{18}F-L-DOPA administered intravenously 45 min before acquisition) was performed using a hybrid machine (Gemini GXL, Philips Medical Systems). The positron emission tomography scan was performed under general anesthesia and glucose infusion to maintain normoglycemia after 6-h fasting and without stopping medications.

Expression of K_{ATP} channels in COSm6 cells. COSm6 cells were cultured in Dulbecco's modified Eagle medium plus 10 mmol/l glucose and supplemented with FCS (10%). Cells were transfected with cDNA using FuGENE 6 Transfection Reagent (Roche Diagnostics, Indianapolis, IN) and then plated on sterile glass coverslips overnight prior to patch-clamp experiments.

Electrophysiological methods. Patch-clamp experiments were performed at room temperature on COSm6 cells that fluoresced green under ultraviolet illumination at 3–5 days post-transfection. Membrane patches were voltage-clamped using an Axopatch 1-D amplifier (Axon Instruments, Union City, CA). All currents were measured at a membrane potential of −50 mV. Data were collected using the pClamp8.2 software suite (Axon Instruments, Union City, CA) and Microsoft Excel. Bath and pipette control solutions (K_{INT}) contained (mM): 150 KCl, 10 HEPES, and 1 EGTA (pH 7.4). Where indicated, ATP was added to the bathing solution as dipotassium salts. Tolbutamide was dissolved in K_{INT} from a 100 mmol/l stock solution in 100 mmol/l KOH.

Macroscopic $^{86}Rb^+$ efflux assays. COSm6 cells in 12-well plates were incubated for 24 h in culture medium containing ^{86}RbCl (1 μCi/ml) 2 days after transfection. Cells were washed twice with Ringer's solution (Basal) (in mM: 118 NaCl, 2.5 $CaCl_2$, 1.2 KH_2PO_4, 4.7 KCl, 25 $NaHCO_3$, 1.2 $MgSO_4$, 10 HEPES; pH 7.4) with or without metabolic inhibition (1 mmol/l 2-deoxy-D-glucose and 2.5 μg/ml oligomycin). At selected time points, solution was removed and replaced with fresh solution; after completion of the assay, cells were lysed with 1% SDS and removed. Collected samples were assayed in a scintillation solution. Raw data are shown as percent $^{86}Rb^+$ efflux relative to total content.

The rate constant of K_{ATP}-specific $^{86}Rb^+$ efflux (k_2) was obtained by fitting a single exponential equation:

$$\text{Relative flux} = 1 - \exp[-(k_1 + k_2) * t] \quad (1)$$

where apparent rate constant for nonspecific efflux (k_1) was obtained from untransfected cells. Glibenclamide was added to Ringer's solution plus metabolic inhibition from a 1 mmol/l stock solution in DMSO. Results are presented as mean ± SEM. Statistical tests and *P* values are noted in the figure legends where appropriate.

Estimation of $P_{o,zero}$ using noise analysis. Mean $P_{o,zero}$ was estimated from stationary fluctuation analysis of macroscopic currents in isolated membrane patches (10,11). Short (<1 s) recordings of currents were analyzed in zero [ATP] and in 5 mmol/l [ATP] (for estimation of ATP-independent noise). Currents were filtered at 1 kHz and digitized at 3 kHz with 12-bit resolution. Mean patch current (I), and variance (σ) in the absence of ATP were obtained by subtraction of mean current and variance in 5 mmol/l ATP (i.e., assuming all channels fully closed). Single-channel current (i) was assumed to be −3.75 pA at −50 mV, corresponding to wild-type (WT) single-channel conductance of 75 pS (12). $P_{o,zero}$ was then estimated from the following equation:

$$P_{o,zero} = 1 - [\sigma^2/(i * I)] \quad (2)$$

Quantitative analysis of ATP inhibition. The ATP dose–response was quantified by fitting the raw data with a Hill equation:

$$I_{rel} = 1/(1 + \{[ATP]/k_{1/2}\}^H) \quad (3)$$

where I_{rel} is the current relative to that in the absence of ATP, [ATP] is the ATP concentration, $k_{1/2}$ is the half-maximal inhibitory ATP concentration, and *H* is the Hill coefficient that was fixed at 1.3.

Immunoblotting. At 48-h post-transfection, cells were washed twice with cold PBS (137 mmol/l NaCl, 2.7 mmol/l KCl, 10 mmol/l Na_2HPO_4, 2 mmol/l KH_2PO_4) and then incubated at 4°C in 300 μl of lysis buffer (150 mmol/l NaCl, 20 mmol/l HEPES, 10 mmol/l EDTA, 1% NP-40, one "Complete Mini" protease inhibitor [Roche Diagnostics, Indianapolis, IN] per 10 ml at pH 7). Lysates were centrifuged for 5 min at 13,000 rpm in 4°C and then transferred to clean microcentrifuge tubes, resolved with SDS-PAGE (7.5% acrylamide), and transferred to polyvinylidene fluoride membranes presoaked in methanol. Filters were blocked overnight in TBS-T (Tris-buffered saline with Tween) buffer (200 mmol/l NaCl, 20 mmol/l Tris-HCl, 0.1% Tween, pH 7.4) plus 5% nonfat dry milk at 4°C. Filters were incubated and rocked for 1 h in a 1:1,000 dilution of anti-SUR1 antibody (affinity-purified from rabbit) in TBS-T plus 5% milk, washed 3 times for 5 min each in TBS-T, then bathed in 1:1,000 dilution of secondary antibody (goat, anti-rabbit IgG, horseradish peroxidase–linked [Pierce]) in TBS-T plus 5% milk. Filters were washed an additional 3 times in TBS-T for 5 min each before appliance of an enhanced chemiluminescence system for detection of horseradish peroxidase (SuperSignal West Pico Chemiluminescent Substrate) and subsequent exposure to autoradiography film (Midwest Scientific, St. Louis, MO).

RESULTS

Genetic pedigree of HI in two separate families with V290M mutation. Figure 1 shows available pedigrees for two families in which the neonatal probands were clinically diagnosed with HI. Proband 1 (female, gestation 38 weeks, birth weight [BW] 3.5 kg, 75–90th centile [13]) was referred by an outside hospital at 2 weeks for evaluation of persistent hypoglycemia (blood glucose <30 mg/dl), despite initiation of dextrose-containing intravenous fluids and diazoxide (15 mg/kg/day). Genotyping (Athena Diagnostics) identified homozygous V290M mutation in *KCNJ11* in the proband and heterozygous V290M in each of the unaffected mother (gestation 40 weeks, BW 3.9 kg, 75–90th centile), father (gestation 40 weeks, BW 4.5 kg, 95–97th centile), and male sibling (gestation 35 weeks, BW 3.0 kg, 75–90th centile), but not in an unaffected male sibling (gestation 36 weeks, BW 2.7 kg, 25–50th centile). Additional sequencing revealed no coding mutations in *GCK*, *GLUD1*, or *ABCC8* genes in the proband. The ancestors of the mother and father came from the same small town in Germany, suggesting the same founder mutations. There is a family history of type 2 diabetes in two maternal great-aunts and a paternal great-grandmother, but no family history of frank hypoglycemia.

Proband 2 was a female born at 38-weeks' gestation (BW 3.4 kg, 75–90th centile) to an Italian family and had the first episode of hypoglycemia at day of life (DOL) 2 (blood glucose 29 mg/dl, treated with glucose infusion). She was referred at 8 weeks to Bambino Gesù Pediatric Hospital for diffuse cyanosis and tremor; plasma glucose was 40 mg/dl with simultaneously elevated insulin of 215 pmol/l and low free fatty acids (220 mmol/l). Diazoxide therapy (15 mg/kg/day) was started and then tapered to 4 mg/kg/day. Genotyping identified heterozygous V290M mutation in *KCNJ11* in both the proband and the apparently unaffected father (not available for further testing). Additional sequencing of proband DNA revealed no coding mutations in *ABCC8*, *GCK*, or *HNF4α* genes.

Variable clinical presentation. Shortly after birth, proband 1 developed cyanosis, blood glucose <20 mg/dl, and was transferred to neonatal intensive care at an outside hospital. The presence of a heart murmur on DOL 2 prompted an echocardiogram (ECHO) that detected a small patent ductus arteriosus, which resolved spontaneously. Despite frequent breast-feeding, supplemental, and

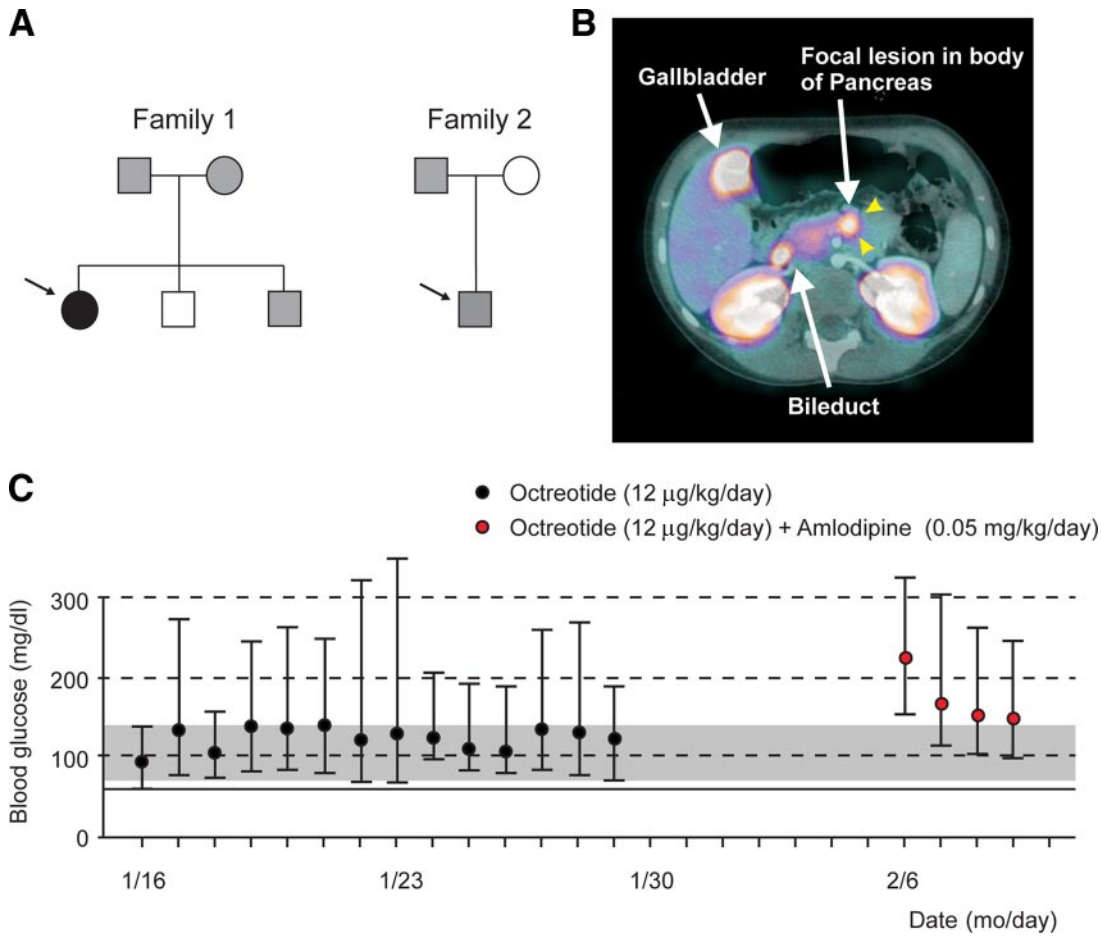

FIG. 1. V290M pedigrees and clinical responses to therapy. *A*: Arrow indicates the V290M proband in each case; black, gray, and empty symbols indicate genetically homozygous, heterozygous, and unaffected individuals, respectively. *B*: Results of fluoro-DOPA scan of proband 2 indicates focal lesion (*yellow arrowheads*) in the body of the pancreas. *C*: Mean daily glucose levels and SD for final period on octreotide alone (8 μg/kg/day divided every 6 h), following switch to octreotide 8 μg/kg/day divided every 6 h plus amlodipine (0.1 mg/kg/day divided every 12 h). Gray area represents target range for alarm for CGMS (70–140 mg/dl glucose). mo, month. (A high-quality digital representation of this figure is available in the online issue.)

intravenous feeds, hypoglycemic episodes (<30 mg/dl) continued. Diazoxide treatment was initiated at 15 mg/kg/day on DOL 10. Laboratory assessment prior to initiation of diazoxide revealed insulin levels of 56 and 70 pmol/l on two occasions when blood glucose was <40 mg/dl. Pituitary testing at the time of hypoglycemia showed intact counterregulatory responses (not shown). In family 2, both the proband and the father carry the V290M mutation in *KCNJ11*, yet only the proband suffers from HI. Lack of mutations in other candidate genes suggested paternal uniparental disomy with loss of heterozygosity of the maternal allele, characteristic of focal HI (14). Fluoro-DOPA scanning (Fig. 1*B*) provided clear evidence of a focal lesion in the body of the pancreas. Extemporary histological examination performed during surgery revealed focal adenomatous hyperplasia of islet cells, prompting complete excision of the lesion and effectively curing the patient and providing further corroborative evidence of focal HI.

Clinical course and treatment experience in proband 1. At DOL 16, proband 1 was transferred to the University of North Carolina Children's Hospital. Blood glucose was <40 mg/dl, and the patient was still receiving diazoxide. In addition, the repeat insulin level was 42 pmol/l with blood glucose of 38 mg/dl. She was started on subcutaneous octreotide (4 μg/kg/day given in divided doses every 8 h). Due to persistent hypoglycemia and concomitant tachyphlyaxis, which is commonly found with octreotide (15), dosing was increased steadily to 12 μg/kg/day (divided doses every 6 h). Diazoxide was tapered off and fasting blood glucose was maintained at >60 mg/dl. On DOL 21, ECHO revealed systolic murmur, mild/moderate left ventricular hypertrophy (LVH), and mild hypertension for age (blood pressure 80–90 mmHg [systolic]/30–40 mmHg [diastolic]). Consequently, amlodipine (0.1 mg/kg/day given in divided dosing twice daily orally) was initiated to treat both LVH and associated hypertension. The repeat ECHO at DOL 46 was normal.

CGMS evaluation. Proband 1 is currently 6-years-old with normal A1C (5.6%), impaired fasting glucose-1 (123 ng/ml), Insulin-like growth factor BP3 (4.3 μg/ml), and serum insulin (119 pmol/l) at ambient glucose of 78 mg/dl. Growth is steady between the 25–50 percentile on octreotide (now 8 μg/kg/day divided 4 times daily). Historically, she was allowed to outgrow her amlodipine. Due to the desire to decrease the frequency of injections, reintroduction of amlodipine was evaluated systematically using CGMS (CareLink, Medtronic) (RESEARCH DESIGN AND METHODS).

Given the long-standing debate as to the usefulness of calcium channel antagonists in HI treatment (16,17), CGMS also permitted ascertaining the response to amlo-

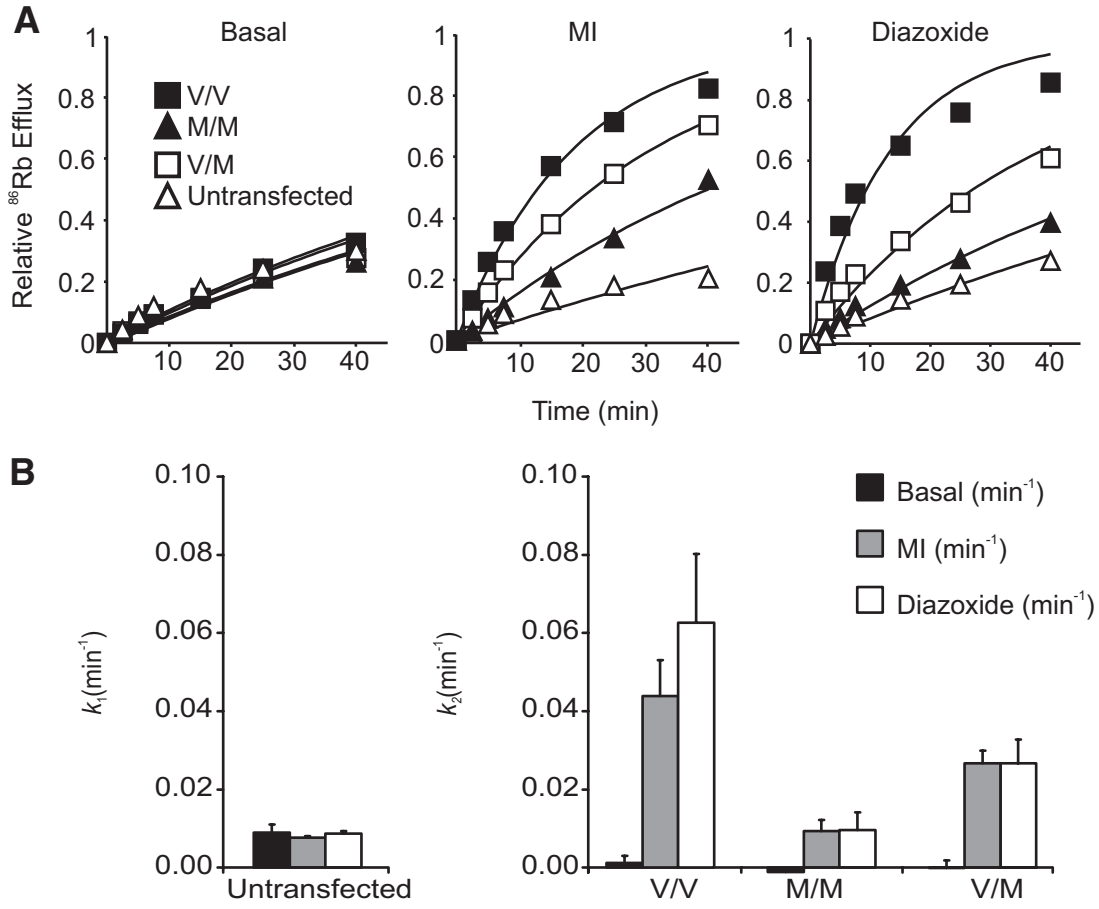

FIG. 2. Decreased K_{ATP} activity in homomeric V290M channels (M/M) and intermediate activity with heteromeric WT and V290M channels (V/M) relative to wild-type (V/V) channels. *A*: Representative ^{86}Rb+ efflux shown as cumulative counts relative to total counts as a function of time, under basal conditions, in the presence of MI, or the presence of K_{ATP} channel opener diazoxide. *B*: Data were fit to a single exponential, and rate constants were obtained from untransfected cells, k_1, for non-K_{ATP} channel ^{86}Rb+ leak and from transfected cells, k_2, for K_{ATP} channel–mediated ^{86}Rb+ current. Graphs show compiled data (mean ± SEM) from 4 to 6 experiments.

dipine, which may inhibit insulin release through direct inhibition of β-cell calcium channels (18) and/or via inhibition of these channels through decreases in cyclic AMP (19). The additive effects of amlodipine plus octreotide therefore would be expected to help to minimize the peak/trough effects of each individual agent. As shown in Fig. 1*C*, octreotide alone maintained average blood glucose levels in the desired range, but marked excursions were still present with episodes >300 mg/dl. There was only one episode of blood glucose <60 mg/dl in >3,000 sensor readings (Fig. 1*B*). Following the introduction of amlodipine, baseline mean blood glucose rose and stabilized at a higher level than with octreotide alone, and there were no episodes of blood glucose levels <60 mg/dl in the presence of octreotide plus amlodipine. Subsequent introduction of bedtime cornstarch further improved control without dangerous excursions but was not tolerated due to typical side effects of bloating and abdominal discomfort, and it was discontinued.

Effect of V290M mutation on K_{ATP} channels expressed in COSm6 cells. To examine the mutation effects on K_{ATP} channel activity, we measured $^{86}Rb^+$ efflux across the plasma membrane of COSm6 cells cotransfected with SUR1, and WT Kir6.2, Kir6.2[V290M], or 1:1 mixture of these subunits. Efflux curves were fit with the two-pathway model (RESEARCH DESIGN AND METHODS), untransfected cells providing the efflux rate (k_1) for the non-K_{ATP} pathway. Homomeric Kir6.2[V290M] (M/M) channels show considerably reduced ^{86}Rb efflux rates, with k_2 reduced by ~80% under metabolically inhibited or diazoxide-stimulated conditions (Fig. 2). Cells expressing heteromeric WT plus V290M (V/M) channels show intermediate efflux rates (k_2, reduced by ~50%) (Fig. 2*B*). These data confirm that the V290M mutation results in reduced K_{ATP} channel activity in intact cells and predict that insulin hypersecretion will be seen in vivo for heterozygous carriers and more severely so in the homozygous state.

Inactivating phenotype of V290M channels. Lysates of COSm6 cells expressing recombinant channels were assayed by immunoblotting (Fig. 3*A*). Anti-SUR1 blots show a doublet at ~170 kDa, corresponding to SUR1 protein, with a similar fraction of complex-glycosylated SUR1 to WT, indicating that the lower activity observed in V290M channels is not due to reduced channel density at the surface of the plasma membrane.

The activity of WT and mutant K_{ATP} channels was further examined in inside-out membrane patch-clamp experiments (Figs. 3–5). Upon membrane excision, WT channels typically open to a steady-state level with open probability of 0.3–0.5 (20). In marked contrast, V290M channels open but then exhibit a rapid decay in macroscopic current, typically resulting in much smaller steady-state currents than is observed in WT channels. Following

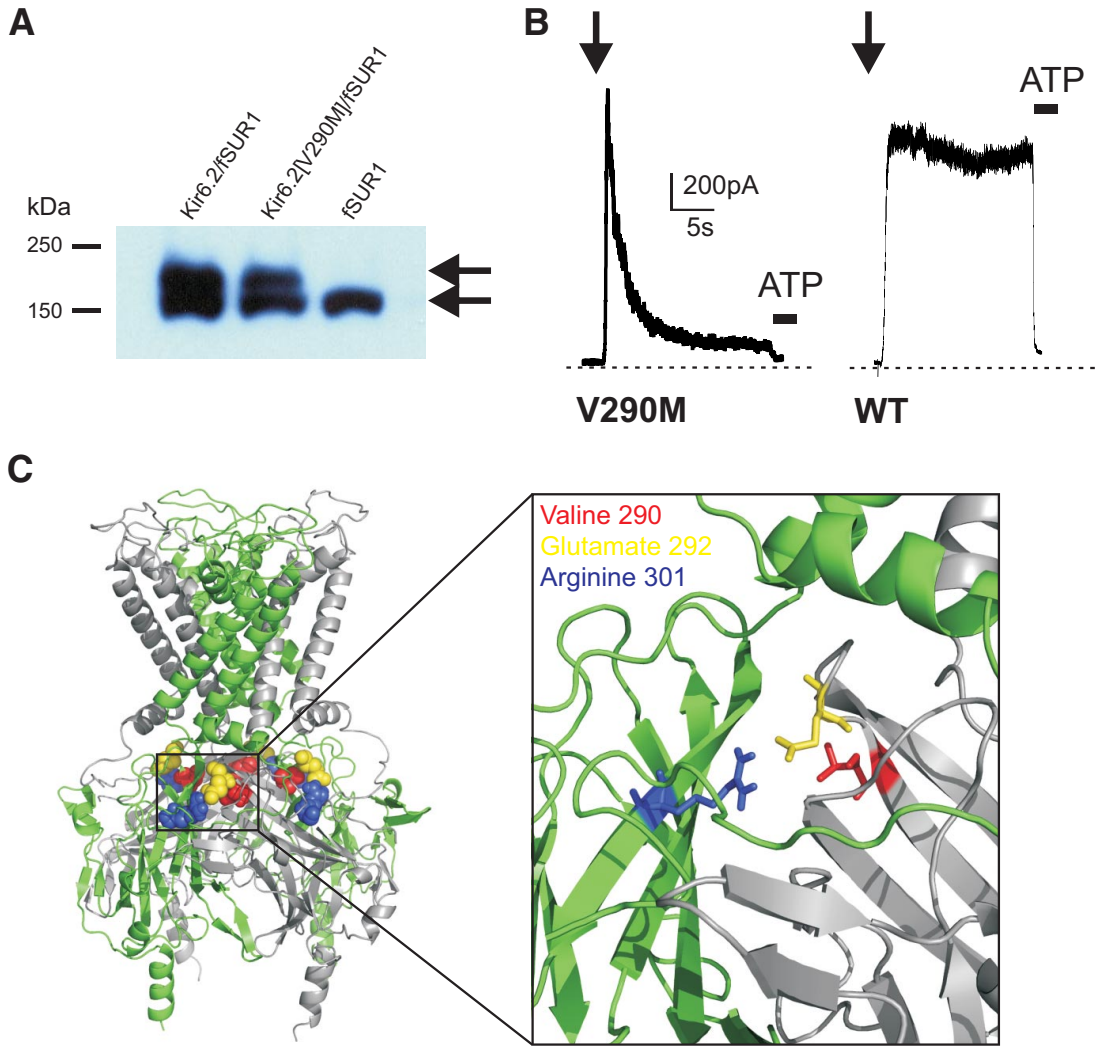

FIG. 3. Molecular basis of loss of K_{ATP} activity. *A*: Western blots of FLAG-tagged SUR1 (fSUR1) from COSm6 cells expressing fSUR1 alone, or co-expressing fSUR1 with either WT Kir6.2 or mutant Kir6.2[V290M]. The mature (cell surface) complex-glycosylated and immature core-glycosylated fSUR1 bands are indicated by upper and lower arrows, respectively. In the absence of Kir6.2, fSUR1 is exclusively core glycosylated. *B*: Representative currents recorded by inside-out excised patch-clamp technique from COSm6 cells expressing WT or mutant V290M K_{ATP} channels at −50 mV membrane potential (+50 mV pipette). Patches were excised from the cell (*arrow*) into zero ATP solution, then subsequently exposed to 5 mmol/l ATP. *C*: Structural model of Kir6.2 tetramer (46) indicates location of V290. R301 and E292 of adjacent Kir6.2 subunits form a salt bridge that is essential for channel function. V290 lies within seven angstroms of R301, and mutations at this site may destabilize the intersubunit interface. (A high-quality digital representation of this figure is available in the online issue.)

patch excision, V290M channels inactivated with time constant of 2.0 ± 0.5 s (n = 5), while WT channels showed essentially no inactivation following excision (Fig. 3*B*). Steady-state ATP sensitivity of V290M channels was similar to WT (Fig. 4*A* and *C*), but current density was considerably lower than WT (Fig. 4*B*), reflecting the dramatic inactivation that occurs. Physiologically, the major determinant of channel activation is stimulation by Mg-nucleotides and, as shown in Fig. 4*D*, MgADP activation is intact in V290M channels, although inactivation follows the MgADP activation, reducing steady-state currents in MgADP.

PIP_2 rescues channels from the inactivated state. Following patch excision, exogenously applied phosphatidylinositol bisphosphate (PIP_2) incorporates into the membrane inner leaflet and typically increases activity of WT channels by two- to threefold as a result of increased open-state stability (21,22) (Fig. 5). Following inactivation to steady-state levels, application of PIP_2 to V290M patches caused much greater relative increase in current (~50-fold) to 1902.58 ± 560.63 pA (n = 8), similar to the WT patch current on excision. During PIP_2 exposure, inactivation became progressively slower and less complete in response to application and removal of ATP (Fig. 5*B*). During this process, the rate and extent of inactivation both decreased in correlation with the estimated open probability (Fig. 6*A*) as expected for an inactivation process occurring from the closed state (DISCUSSION).

OGTT evaluation in heterozygous carriers in family 1. In mouse models of reduced K_{ATP}, even 50% reduction is sufficient to cause enhanced glucose tolerance and hypersecretion of insulin (23,24). Given that heteromeric V290M/WT channels exhibit ~50% reduction of K_{ATP} conductance (Fig. 2) and the anecdotal evidence of hypersensitivity to glucose exhibited by the proband's brother, we pursued OGTT in the mother (Table 1) and the brother (Table 2), both of whom are heterozygous for the V290M mutation. Blood glucose in healthy adults will be below 200 mg/dl at 1 h and below 140 mg/dl at 2 h; in healthy children, it will be ~100 mg/dl at 1 h (25).

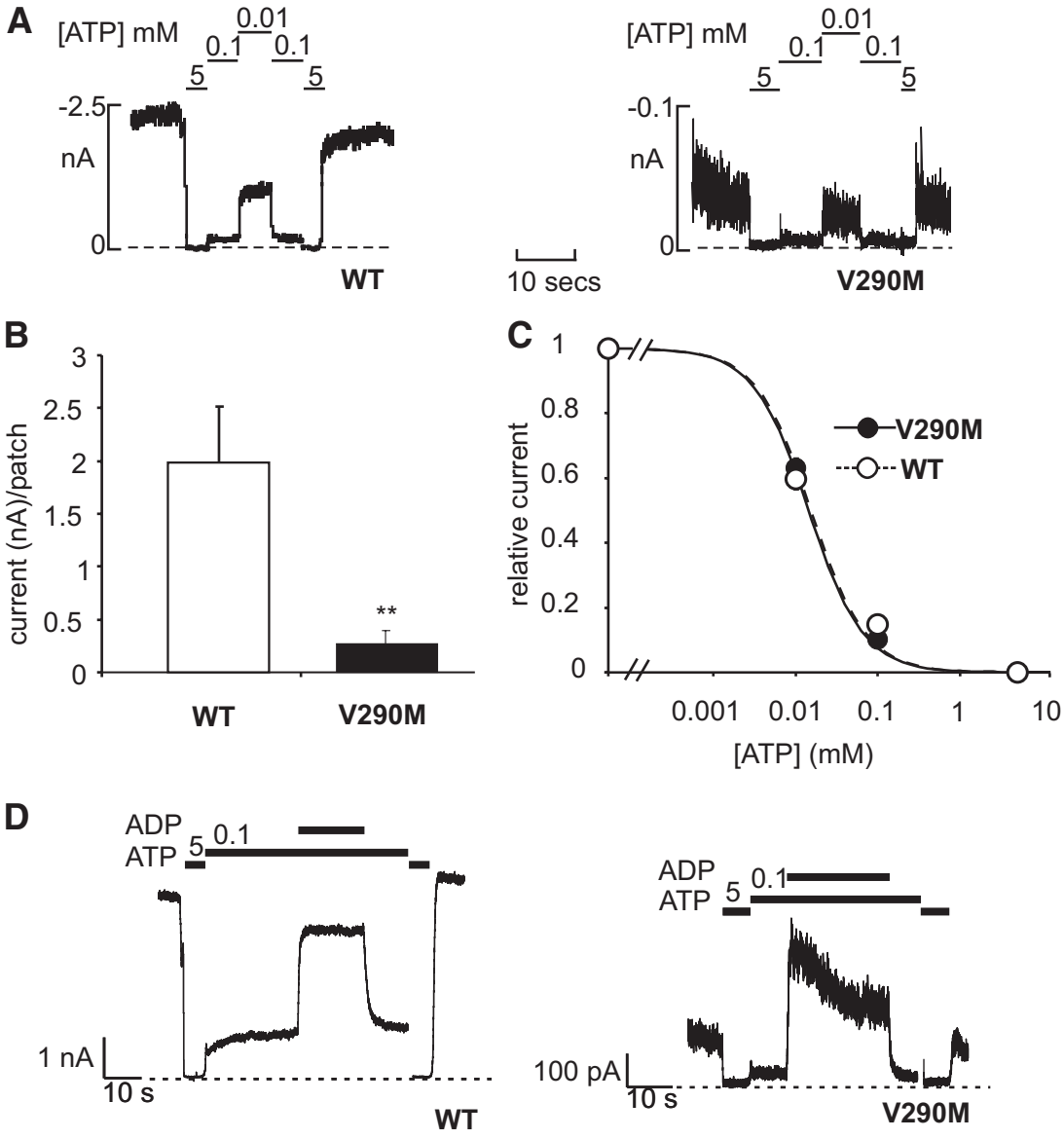

FIG. 4. Mutant V290M channels have unaltered ATP-sensitivity and intact MgADP activation. *A*: Representative currents recorded by inside-out excised patch-clamp technique from COSm6 cells expressing WT or mutant V290M K_{ATP} channels at −50 mV membrane potential (+50 mV pipette). Patches were exposed to different concentrations of ATP as indicated. *B*: Mean steady-state patch current following isolation (± SEM). *C*: Steady-state dependence of membrane current on ATP relative to current in the absence of ATP. Solid line represents mutant V290M channels while dashed line represents WT channels fitted with the Hill equation by least-squares method. *D*: Representative currents recorded by inside-out excised patch-clamp technique from COSm6 cells expressing WT or mutant V290M K_{ATP} channels at −50 mV membrane potential (+50 mV pipette). Patches were exposed to different concentrations of ATP, and ADP (in the presence of 0.5. mM free Mg^{2+}) as indicated.

Even though neither mother nor brother displays overt HI under-fed conditions, glucose was close to fasting levels in both at 1 h, and even lower at 2 h, suggestive of a "supranormal" response. Proinsulin levels rose during OGTT and, although within the reported ranges for healthy subjects (26), proinsulin-to-insulin ratios at 1 and 2 h were above the normal range for young individuals (26).

DISCUSSION

Molecular basis of HI associated with Kir6.2[V290M] mutation. We describe two unrelated families with the Kir6.2[V290M] mutation. By recombinant expression of WT or V290M mutant Kir6.2 subunits, we show that the mutation results in partial loss of K_{ATP} channel activity in the heterozygous case and more severe loss in the homozygous case (Fig. 2). The loss of function results from induction of an inactivation phenomenon (Fig. 3*B*), which is similar to that resulting from HI-associated mutations at Kir6.2 residue R301 (27). These mutations resulted in both loss of functional membrane channels and an inactivating phenotype. The V290M mutation seems to reduce channel activity solely through induction of inactivation since surface expression appears normal (Fig. 3*A*). Structural analysis suggests that V290 participates in the generation of an inter-subunit salt bridge involving R301 and E290 (Fig. 3*C*). We suggest that V290M and R301 mutations induce the same inactivating phenotype by destabilizing this salt bridge, causing the channel to enter a long-lived inactivated state after closure in the absence of ATP. The observed relationship between $K_{1/2,ATP}$ and open probability is an emergent property of gating schemes in which

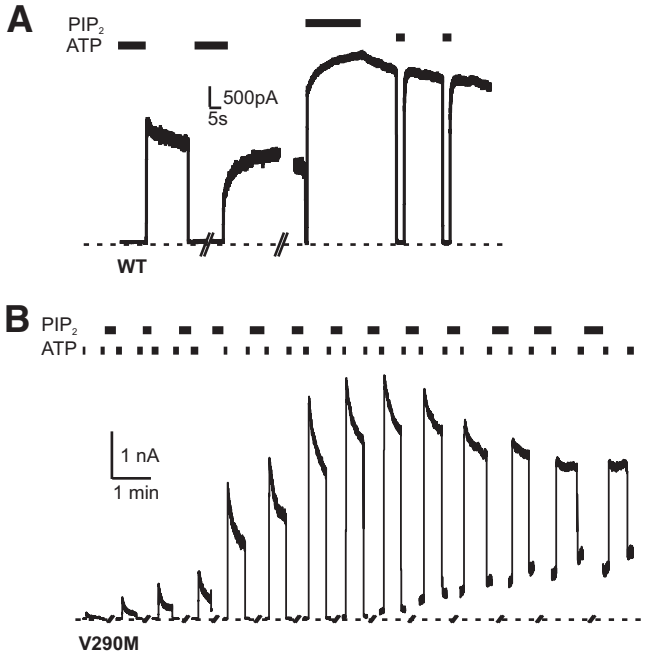

FIG. 5. Inactivation is PIP_2-sensitive. Current recordings of COSm6 patches expressing WT (*A*) and mutant V290M (*B*) channels. In WT channels, the current approximately doubles following addition of PIP_2. However, in V290M channels, steady-state channel activity increases several-fold, accompanied by a marked reduction in inactivation following exposures to PIP_2, a channel open-state stabilizer.

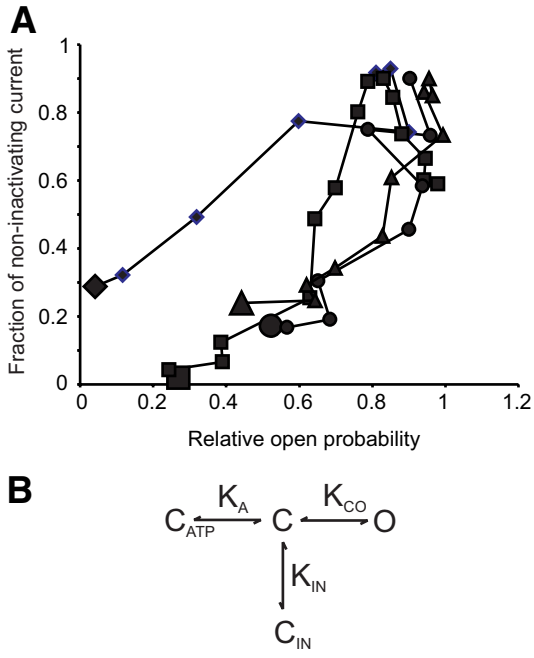

FIG. 6. Kinetic mechanism of inactivation. *A*: Fraction of inactivating current (following ATP removal) vs. steady-state current (relative to maximal attained following repeat PIP_2 exposure–relative open probability) at selected time points following exposures to PIP_2 in V290M channels. Individual patches are indicated by different symbols; large symbols indicate starting values prior to first exposure to PIP_2. *B*: A 3-state model of channel activity (with an unliganded open and closed state, and with ATP binding to the closed state) is adequate to explain multiple features of K_{ATP} gating (28,47,48). A fourth, inactivated, state (C_{IN}), which is coupled to the unliganded closed state, can explain both the phenomenon of inactivation and the finding that PIP_2 (which acts to shift the KCO equilibrium toward the open state) both reduces and slows inactivation.

ATP preferentially stabilizes the closed state of the channel (28), and loss of inactivation paralleling increase in open-state stability with PIP_2 is then predicted by the assumption that inactivation occurs from the unliganded closed state (Fig. 6*B*).

Variable presentation of HI associated with Kir6.2[V290M] mutation. In family 1, HI in the neonatal period is clearly associated with the homozygous condition. In the proband of family 2, the mutation presents in a focal lesion with loss of heterozygosity. K_{ATP} channel activity reduction is graded from the heteromeric to the homomeric expression with severe (>80%) loss in the homomeric case; this is consistent with the clinical HI phenotype of these two probands. In the heterozygous case, reduction of channel activity is ~50%. Previous extensive studies of animal models of genetic suppression of K_{ATP} activity predict that such a reduction is sufficient to cause glucose hyperresponsivity with left-shifted glucose-dependence of insulin secretion, but unaltered basal secretion (29–31). The relevance of this to humans remains unclear, but seems a reasonable explanation for the apparent glucose hyperresponsivity of the two carrier relatives in family 2. In this regard, it is notable that the affected probands in each family and the three unaffected heterozygous carriers in family 1 were at the upper range of normal birthweights and large relative to the unaffected sibling. The anecdotal observation of the mother in family 1 that the 4-year-old heterozygous-carrier child can become hungry and/or lethargic after eating might reflect postprandial hypoglycemia and may warrant caution during meals and/or modification of meal carbohydrate composition for such an individual. There are few published studies focusing on heterozygous carriers of HI mutations. Huopio et al. (32) reported that carriers of the SUR1 V187D mutation had normal glucose tolerance and insulin secretory capacity. However, V187D reduces K_{ATP} channel activity by affecting trafficking to the surface membrane, and this is readily reversible, even simply by exposure to sulfonylureas (33). It is unclear whether the presence of even a single WT subunit might be sufficient for normal trafficking in the heterozygous case, such that there is minimal effect on K_{ATP} density in heterozygous carriers. Otherwise, for recessive loss of function HI mutations that do cause reduction in channel density in the heterozygous case, it seems that glucose hyperresponsivity might be a feature, although clearly this requires further study in bigger cohorts.

There are now several reports of patients with HI due to loss-of-function K_{ATP} mutations "crossing-over" to diabetes in later life, including heterozygous carriers of SUR1 mutations (34,35). Again, this is predicted from mouse models of the loss of K_{ATP} activity (36,31), which become glucose-intolerant as adults and diabetic on high-fat diets.

TABLE 1
OGTT in heterozygous mother

Time	Serum glucose (mg/dl)	Insulin (pmol/l)	Proinsulin (pmol/l)	Proinsulin-to-insulin ratio
Baseline	82	40.6	3.4	0.083:744
1 h	75	350	17	0.048:571
2 h	74	133	13	0.097:744
3 h	63	14	6.7	0.478:571
4 h	72	9.1	4.7	0.516:484
5 h	73	6.3	3.1	0.492:063

TABLE 2
OGTT in heterozygous brother

Time	Serum glucose (mg/dl)	Insulin (pmol/l)	Proinsulin (pmol/l)	Proinsulin-to-insulin ratio
Baseline	77	35	4.2	0.12
1 h	90	280	15	0.053:571
2 h	79	54.6	11	0.201:465
3 h	66	18.2	5.7	0.313:187

It is notable that the proinsulin-to-insulin levels in the heterozygous carriers were in the normal range (0.1–0.2) in the fasted state and fell appropriately in the first hour of the OGTT, but then rose to relatively higher levels at 2 and 3 h than has been reported for healthy young subjects, and reminiscent of the elevated ratios seen in type 2 diabetics (26,37). Conceivably, this apparently elevated proinsulin-to-insulin ratio reflects so-called β-cell overwork and might be a harbinger of a tendency to crossover later in life.

Treatment options for K_{ATP}-dependent HI. Standard treatment options for HI are essentially limited to diazoxide (activating K_{ATP} and suppressing insulin secretion) or octreotide (long-acting somatostatin analog suppressing glucose actions on the β-cell), glucagon (counterregulator to insulin) or subtotal pancreatectomy (17,38–40). L-type (dihydropyridine-sensitive, Ca_V1) channel blockers are mechanistically an attractive option to directly modulate insulin secretion. Previous results have been mixed (16,41), but some patients have achieved stable blood glucose levels on nifedipine monotherapy. In the present case, improvement in both LVH and hypertension in addition to hypoglycemia are shown in a neonate on both amlodipine and octreotide. The contribution of amlodipine to blood glucose was assessed more directly using CGMS when the proband became of school-age. The main finding was a rise in basal glucose levels with no values below 70 mg/dl while on the same dose of octreotide in the presence of amlodipine. Given its mechanism of Ca_v1 channel inhibition, this finding is not surprising and supports the results of Aynsley-Green and colleagues (42). In the present case, amlodipine also permitted extension of octreotide dosing from every 6 h to every 8 h, thereby saving 1 injection daily (a significant improvement in quality of life).

A key clinical management question for HI is whether to pursue medical or surgical therapy. Long-term medical therapy, as in this case, presents a less expensive option than subtotal pancreatectomy, which is the procedure that would be indicated by the mutation and mode of inheritance. In addition, excellent glucose control, normal growth and development, and the variable risk of postsurgical diabetes all support this management to date for this child. Moreover, glucose levels normalize and medical therapy can be stopped at some point for many HI children (41,43–45), whereas patients who undergo major resection of the pancreas will tend to develop diabetes at or around puberty, another consideration when assessing the pros and cons of surgical versus medical management.

We report on HI due to a K_{ATP} mutation that results in an inactivating channel in two different families. A homozygous-affected child is well controlled with medical therapy without surgery. Clinically unaffected heterozygous carriers show signs of hypersecretion, and we suggest that they may represent an unappreciated cohort with subclinical features.

ACKNOWLEDGMENTS

This work was supported by National Institutes of Health Grant DK69445 (to C.G.N.). F.B. is a member of the Early Onset Diabetes Study Group of the Italian Society of Pediatric Endocrinology and Diabetology.

No potential conflicts of interest relevant to this article were reported.

K.J.L., A.A., and J.C.K. researched data and wrote the manuscript. H.T.K., C.D.-V., A.M., M.P., V.R., J.d.V.d.G., and C.C. researched data. F.B. and C.G.N. wrote the manuscript.

We would like to thank Medtronic for both clinical and technical support during the use of CGMS monitoring for the second subject. Human studies for the second patient and family were carried out under the institutional review board exempt category at the University of North Carolina (K.J.L.).

REFERENCES

1. Koster JC, Marshall BA, Ensor N, Corbett JA, Nichols CG. Targeted overactivity of beta cell K(ATP) channels induces profound neonatal diabetes. Cell 2000;100:645–654
2. Gloyn AL, Pearson ER, Antcliff JF, Proks P, Bruining GJ, Slingerland AS, Howard N, Srinivasan S, Silva JM, Molnes J, Edghill EL, Frayling TM, Temple IK, Mackay D, Shield JP, Sumnik Z, van Rhijn A, Wales JK, Clark P, Gorman S, Aisenberg J, Ellard S, Njølstad PR, Ashcroft FM, Hattersley AT. Activating mutations in the gene encoding the ATP-sensitive potassium-channel subunit Kir6.2 and permanent neonatal diabetes. N Engl J Med 2004;350:1838–1849
3. Thomas PM, Cote GJ, Wohllk N, Haddad B, Mathew PM, Rabl W, Aguilar-Bryan L, Gagel RF, Bryan J. Mutations in the sulfonylurea receptor gene in familial persistent hyperinsulinemic hypoglycemia of infancy. Science 1995;268:426–429
4. Nichols CG, Shyng SL, Nestorowicz A, Glaser B, Clement JP 4th, Gonzalez G, Aguilar-Bryan L, Permutt MA, Bryan J. Adenosine diphosphate as an intracellular regulator of insulin secretion. Science 1996;272:1785–1787
5. Huopio H, Shyng SL, Otonkoski T, Nichols CG. K(ATP) channels and insulin secretion disorders. Am J Physiol Endocrinol Metab 2002;283:E207–E216
6. Flanagan SE, Clauin S, Bellanné-Chantelot C, de Lonlay P, Harries LW, Gloyn AL, Ellard S. Update of mutations in the genes encoding the pancreatic beta-cell K(ATP) channel subunits Kir6.2 (KCNJ11) and sulfonylurea receptor 1 (ABCC8) in diabetes mellitus and hyperinsulinism. Hum Mutat 2009;30:170–180
7. Shyng S, Nichols CG. Octameric stoichiometry of the KATP channel complex. J Gen Physiol 1997;110:655–664
8. Inagaki N, Gonoi T, Seino S. Subunit stoichiometry of the pancreatic beta-cell ATP-sensitive K+ channel. FEBS Lett 1997;409:232–236
9. Clement JP 4th, Kunjilwar K, Gonzalez G, Schwanstecher M, Panten U, Aguilar-Bryan L, Bryan J. Association and stoichiometry of K(ATP) channel subunits. Neuron 1997;18:827–838
10. Neher E, Stevens CF. Conductance fluctuations and ionic pores in membranes. Ann Rev Biophys Bioeng 1977;6:345–381
11. Sigworth FJ. The variance of sodium current fluctuations at the node of Ranvier. J Physiol 1980;307:97–129
12. Shyng S, Ferrigni T, Nichols CG. Control of rectification and gating of cloned KATP channels by the Kir6.2 subunit. J Gen Physiol 1997;110:141–153
13. Bonellie S, Chalmers J, Gray R, Greer I, Jarvis S, Williams C. Centile charts for birthweight for gestational age for Scottish singleton births. BMC Pregnancy Childbirth 2008;8:5
14. Glaser B, Ryan F, Donath M, Landau H, Stanley CA, Baker L, Barton DE, Thornton PS. Hyperinsulinism caused by paternal-specific inheritance of a recessive mutation in the sulfonylurea-receptor gene. Diabetes 1999;48:1652–1657
15. Hofland LJ, van der Hoek J, Feelders R, van der Lely AJ, de Herder W, Lamberts SW. Pre-clinical and clinical experiences with novel somatostatin ligands: advantages, disadvantages and new prospects. J Endocrinol Invest 2005;28:36–42
16. Müller D, Zimmering M, Roehr CC. Should nifedipine be used to counter low blood sugar levels in children with persistent hyperinsulinaemic hypoglycaemia? Arch Dis Child 2004;89:83–85

17. Hussain K, Aynsley-Green A. Management of hyperinsulinism in infancy and childhood. Ann Med 2000;32:544–551
18. Malaisse WJ, Boschero AC. Calcium antagonists and islet function. XI. Effect of nifedipine. Horm Res 1977;8:203–209
19. Hansen JB, Arkhammar PO, Bodvarsdottir TB, Wahl P. Inhibition of insulin secretion as a new drug target in the treatment of metabolic disorders. Curr Med Chem 2004;11:1595–1615
20. Nichols CG. KATP channels as molecular sensors of cellular metabolism. Nature 2006;440:470–476
21. Shyng SL, Nichols CG. Membrane phospholipid control of nucleotide sensitivity of KATP channels. Science 1998;282:1138–1141
22. Enkvetchakul D, Nichols CG. Gating mechanism of KATP channels: function fits form. J Gen Physiol 2003;122:471–480
23. Koster JC, Remedi MS, Flagg TP, Johnson JD, Markova KP, Marshall BA, Nichols CG. Hyperinsulinism induced by targeted suppression of beta cell KATP channels. Proc Natl Acad Sci U S A 2002;99:16992–16997
24. Remedi MS, Rocheleau JV, Tong A, Patton BL, McDaniel ML, Piston DW, Koster JC, Nichols CG. Hyperinsulinism in mice with heterozygous loss of K(ATP) channels. Diabetologia 2006;49:2368–2378
25. Knopf CF, Cresto JC, Dujovne IL, Ramos O, de Majo SF. Oral glucose tolerance test in 100 normal children. Acta Diabetol Lat 1977;14:95–103
26. Fritsche A, Madaus A, Stefan N, Tschritter O, Maerker E, Teigeler A, Haring H, Stumvoll M. Relationships among age, proinsulin conversion, and β-cell function in nondiabetic humans. Diabetes 2002;51(Suppl. 1): S234–S239
27. Lin YW, Bushman JD, Yan FF, Haidar S, MacMullen C, Ganguly A, Stanley CA, Shyng SL. Destabilization of ATP-sensitive potassium channel activity by novel KCNJ11 mutations identified in congenital hyperinsulinism. J Biol Chem 2008;283:9146–9156
28. Enkvetchakul D, Loussouarn G, Makhina E, Shyng SL, Nichols CG. The kinetic and physical basis of K(ATP) channel gating: toward a unified molecular understanding. Biophys J 2000;78:2334–2348
29. Koster JC, Remedi MS, Flagg TP, Johnson JD, Markova KP, Marshall BA, Nichols CG. Hyperinsulinism induced by targeted suppression of beta cell KATP channels. Proc Natl Acad Sci U S A 2002;99:16992–16997
30. Remedi MS, Rocheleau JV, Tong A, Patton BL, McDaniel ML, Piston DW, Koster JC, Nichols CG. Hyperinsulinism in mice with heterozygous loss of K(ATP) channels. Diabetologia 2006;49:2368–2378
31. Nichols CG, Koster JC, Remedi MS. β-Cell hyperexcitability: from hyperinsulinism to diabetes. Diabetes Obes Metab 2007;9(Suppl. 2):81–88
32. Huopio H, Vauhkonen I, Komulainen J, Niskanen L, Otonkoski T, Laakso M. Carriers of an inactivating β-cell ATP-sensitive K^+ channel mutation have normal glucose tolerance and insulin sensitivity and appropriate insulin secretion. Diabetes Care 2002;25:101–106
33. Yan F, Lin CW, Weisiger E, Cartier EA, Taschenberger G, Shyng SL. Sulfonylureas correct trafficking defects of ATP-sensitive potassium channels caused by mutations in the sulfonylurea receptor. J Biol Chem 2004;279:11096–11105
34. Huopio H, Reimann F, Ashfield R, Komulainen J, Lenko HL, Rahier J, Vauhkonen I, Kere J, Laakso M, Ashcroft F, Otonkoski T. Dominantly inherited hyperinsulinism caused by a mutation in the sulfonylurea receptor type 1. J Clin Invest 2000;106:897–906
35. Grimberg A, Ferry RJ Jr, Kelly A, Koo-McCoy S, Polonsky K, Glaser B, Permutt MA, Aguilar-Bryan L, Stafford D, Thornton PS, Baker L, Stanley CA. Dysregulation of insulin secretion in children with congenital hyperinsulinism due to sulfonylurea receptor mutations. Diabetes 2001;50:322–328
36. Remedi MS, Koster JC, Markova K, Seino S, Miki T, Patton BL, McDaniel ML, Nichols CG. Diet-induced glucose intolerance in mice with decreased β-cell ATP-sensitive K^+ channels. Diabetes 2004;53:3159–3167
37. Tura A, Pacini G, Kautzky-Willer A, Ludvik B, Prager R, Thomaseth K. Basal and dynamic proinsulin-insulin relationship to assess beta-cell function during OGTT in metabolic disorders. Am J Physiol Endocrinol Metab 2003;285:E155–E162
38. Mazor-Aronovitch K, Landau H, Gillis D. Surgical versus non-surgical treatment of congenital hyperinsulinism. Pediatr Endocrinol Rev 2009;6: 424–430
39. Aynsley-Green A, Hussain K, Hall J, Saudubray JM, Nihoul-Fékété C, De Lonlay-Debeney P, Brunelle F, Otonkoski T, Thornton P, Lindley KJ. Practical management of hyperinsulinism in infancy. Arch Dis Child Fetal Neonatal Ed 2000;82:F98–F107
40. Stanley CA. Hypoglycemia in the neonate. Pediatr Endocrinol Rev 2006; 4(Suppl. 1):76–81
41. Hussain K, Aynsley-Green A, Stanley CA. Medications used in the treatment of hypoglycemia due to congenital hyperinsulinism of infancy (HI). Pediatr Endocrinol Rev 2004;2(Suppl. 1):163–167
42. Lindley KJ, Dunne MJ, Kane C, Shepherd RM, Squires PE, James RF, Johnson PR, Eckhardt S, Wakeling E, Dattani M, Milla PJ, Aynsley-Green A. Ionic control of beta cell function in nesidioblastosis: a possible therapeutic role for calcium channel blockade. Arch Dis Child 1996;74: 373–378
43. Dacou-Voutetakis C, Psychou F, Maniati-Christidis M. Persistent hyperinsulinemic hypoglycemia of infancy: long-term results. J Pediatr Endocrinol Metab 1998;11(Suppl. 1):131–141
44. Hussain K, Aynsley-Green A. Management of hyperinsulinism in infancy and childhood. Ann Med 2000;32:544–551
45. Arnoux JB, de Lonlay P, Ribeiro MJ, Hussain K, Blankenstein O, Mohnike K, Valayannopoulos V, Robert JJ, Rahier J, Sempoux C, Bellanné C, Verkarre V, Aigrain Y, Jaubert F, Brunelle F, Nihoul-Fékété C. Congenital hyperinsulinism. Early Hum Dev 2010;86:287–294
46. Antcliff JF, Haider S, Proks P, Sansom MS, Ashcroft FM. Functional analysis of a structural model of the ATP-binding site of the KATP channel Kir6.2 subunit. EMBO J 2005;24:229–239
47. Enkvetchakul D, Loussouarn G, Makhina E, Nichols CG. ATP interaction with the open state of the K(ATP) channel. Biophys J 2001;80:719–728
48. Enkvetchakul D, Nichols CG. Gating mechanism of KATP channels: function fits form. J Gen Physiol 2003;122:471–480